

# Magnetic Field Induced Morphological Transitions in Block Copolymer/Superparamagnetic Nanoparticle Composites

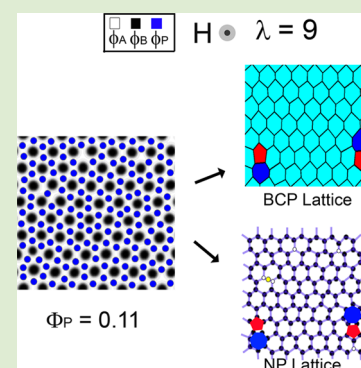
Vinay Raman,<sup>†</sup> Ravi Sharma,<sup>‡</sup> T. Alan Hatton,<sup>\*,†</sup> and Bradley D. Olsen<sup>\*,†</sup>

<sup>†</sup>Department of Chemical Engineering, Massachusetts Institute of Technology, Cambridge, Massachusetts 02139, United States

<sup>‡</sup>Cabot Corporation, 157 Concord Road, Billerica, Massachusetts 01821, United States

## S Supporting Information

**ABSTRACT:** This two-dimensional computational study investigates the effect of external magnetic fields on thin film nanocomposites comprised of superparamagnetic nanoparticles dispersed within block copolymer melts, which display a variety of morphological transitions based on the field orientation, nanoparticle loading, and selectivity of the nanoparticles for the blocks. In-plane magnetic fields lead to chaining of the nanoparticles; when selective for the minority block in a hexagonal block copolymer nanostructure, this chaining results in the formation of stripe phases oriented parallel to the magnetic field. When selective for the majority block of the hexagonal structure, nanoparticle chains of sufficient persistence length drive the orientation of the hexagonal morphology with the  $\langle 100 \rangle$  direction oriented parallel to the magnetic field. Out-of-plane magnetic fields induce repulsive dipolar interactions between the nanoparticles that annihilate the defects in the hexagonal morphology of the block copolymer when the nanoparticle is selective for the minority block. When the nanoparticles are selective for the majority block and the field is oriented out of plane, repulsive dipolar interactions lead to the formation of honeycomb lattices. In all cases, the nanoparticle size and volume fraction must be chosen to maximize the commensurability with the block copolymer structure to optimize the ordering of the final composite.



Block copolymer nanocomposites are an interesting class of heterogeneous materials that are known for their enhanced mechanical, optical and electrical properties; the characteristics of the nanoparticles play an important role in determining the morphology and properties of the composites.<sup>1,2</sup> Block copolymer self-assembles into morphologies such as lamellae, spheres, and cylinders that can be used to achieve a preferred spatial and orientational distribution of nanoparticles.<sup>2,3</sup> The morphology of the block copolymer nanocomposites has an effect on the optical<sup>4,5</sup> and mechanical performance<sup>6</sup> of nanocomposites.

The morphology of block copolymer nanocomposites depends on the interplay of nanoparticle size, nanoparticle loading, and particle selectivity for the blocks, as is evident from the results of many theoretical<sup>7–11</sup> and experimental<sup>12,13</sup> studies on the phase behavior of block copolymer–nanoparticle mixtures. The presence of nonselective nanoparticles in the block copolymers, for example, affects the order–disorder transition (ODT) temperature,<sup>14,15</sup> effectively reducing the Flory–Huggins interaction energy of the two blocks due to the losses in conformational entropy of the polymer chains.<sup>14</sup> Excluded volume interactions between the nanoparticles and the block copolymer also lead to morphological transitions due to the swelling of the block copolymer domains.<sup>16,17</sup> Morphology control of composites can be achieved by tuning the enthalpic and entropic interactions between the nanoparticles and the block copolymer. Enthalpic interactions, for instance, can be tuned by functionalization of nanoparticle

surfaces with selective or nonselective ligands, while entropic interactions are known to depend on the size of the nanoparticles relative to the block copolymer domain spacing.<sup>18</sup> Confinement effects<sup>19</sup> and substrate chemical potentials<sup>20</sup> are also known to play an important role in the self-assembly of these composite systems due to both symmetry breaking and surface segregation of polymer or nanoparticles to the confining interface.<sup>19</sup> Interparticle interactions between the nanoparticles can also affect the morphology of the composite,<sup>21</sup> and control of interparticle interactions<sup>22</sup> can serve as an efficient tool to manipulate the hierarchical assembly of block copolymers, especially when long-range interactions are present.

In block copolymer nanocomposites with magnetic nanoparticles, uniform magnetic fields can be used to alter the orientation of magnetic nanoparticle dipoles<sup>23</sup> and consequently tune the long-range interparticle interactions. This affects the structure of nanoparticle aggregates and subsequently the morphology of the block copolymer nanocomposite. For instance, magnetic nanoparticles are known to form chain-like aggregates due to dipolar interactions that are predicted to promote alignment of block copolymer nanostructures.<sup>21,24</sup> He and Balazs<sup>21</sup> demonstrated using cell dynamics simulations that in-plane magnetic fields promote alignment of magnetic nanoparticles and, consequently,

Received: May 15, 2013

Accepted: July 12, 2013

Published: July 16, 2013

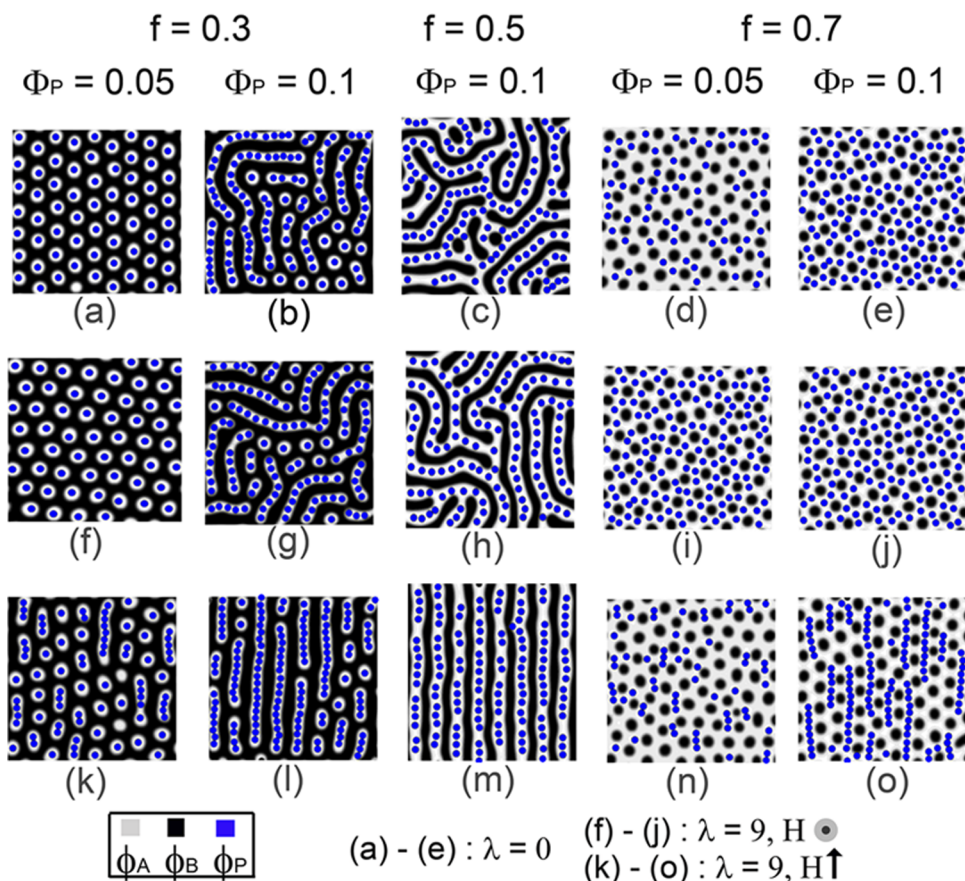


**Figure 1.** Effect of dipolar interactions on the morphology of the block copolymer nanocomposite,  $R_p = 0.5R_g$ ,  $\chi_{BP}N = 30$ ; (a–e) nonmagnetic nanoparticles; (f–j) magnetic field ( $\vec{H}$ ) is out-of-plane (along  $z$ -axis); (k–o) magnetic field ( $\vec{H}$ ) is in-plane (along  $y$ -axis). Local volume fractions for block A (bright regions), B (dark regions), and nanoparticles (blue spheres) are represented by  $\phi_A$ ,  $\phi_B$ , and  $\phi_P$ , respectively;  $\lambda$  represents the ratio of dipolar interaction energy to thermal energy.

alignment of lamellar domains as well as cylinder-forming block copolymers. Recently, we studied the effect of chaining of superparamagnetic nanoparticles on the alignment of symmetric block copolymers using hybrid particle-field theory simulations, which explicitly took into account the excluded volume interactions between the nanoparticles and the block copolymer. We delineated the role of dipolar interaction strength, nanoparticle size, nanoparticle loading, and the surface interaction of the nanoparticles with the block copolymer on the morphology of the composite.<sup>24</sup>

While previous modeling efforts have focused primarily on in-plane magnetic fields which lead to the formation of superparamagnetic nanoparticle chains, out-of-plane magnetic fields can change the symmetry of the nanoparticle aggregates to form hexagonal arrays due to repulsive dipolar interactions. In this Letter, we investigate the interplay of magnetic field orientation, coil fraction of the block copolymer, nanoparticle size and loading on the morphology of the composite, specifically exploring the interplay between block copolymer and superparamagnetic nanoparticle lattice symmetry. Depending upon the symmetry of the block copolymer in two-dimensional simulations (hexagonal/dots and lamellar/stripes), the nanoparticles induce a variety of morphological transitions in the final composite.

The effects of nanoparticle size and loading on the self-assembly of the composite system are characterized using a hybrid of self-consistent field theory (SCFT) and Brownian dynamics.<sup>17,24</sup> The block copolymer is characterized by the coil

fraction,  $f$ , of the block that has the most favorable interaction with the nanoparticles. The Flory–Huggins interaction parameter between the blocks is denoted by  $\chi_{AB}$ , while the selectivities of the nanoparticles for the two blocks A and B are denoted by  $\chi_{AP}$  and  $\chi_{BP}$ , respectively.  $N$  is the total degree of polymerization of the block copolymer chain. All of the Flory–Huggins interaction parameters were kept fixed ( $\chi_{AP}N = 0$ ,  $\chi_{BP}N = 30$ ,  $\chi_{AB}N = 20$ ) in the simulations. All lengths (box size  $L$  and the nanoparticle radius,  $R_p$ ) are scaled by  $R_g$ , the unperturbed radius of gyration of the block copolymer. The statistical segment lengths of the A and B blocks are assumed to be equal, and the overall nanoparticle volume fraction is denoted by  $\Phi_P$ . The dipolar interactions are characterized by the parameter  $\lambda$ , the ratio of the dipolar interaction energy to the thermal energy ( $k_B T$ ). The dipole moments are assumed to align in the direction of the applied magnetic field, a valid assumption when the external magnetic field strength is much larger than the saturation magnetization strength of the nanoparticle. Since the simulations are in two dimensions, the symmetric block copolymers form phases with line symmetry (referred to as stripe phases), and the asymmetric block copolymers form hexagonal phases (referred to as dot phases). For the case of assembly in thin films, stripe phases can be identified with lamellar phases or cylinders oriented parallel to the surface of the film, while dot phases are akin to spherical phases or perpendicularly oriented cylinders.

The simulations reveal that dipolar interactions have a significant influence on the morphology of the block copolymer

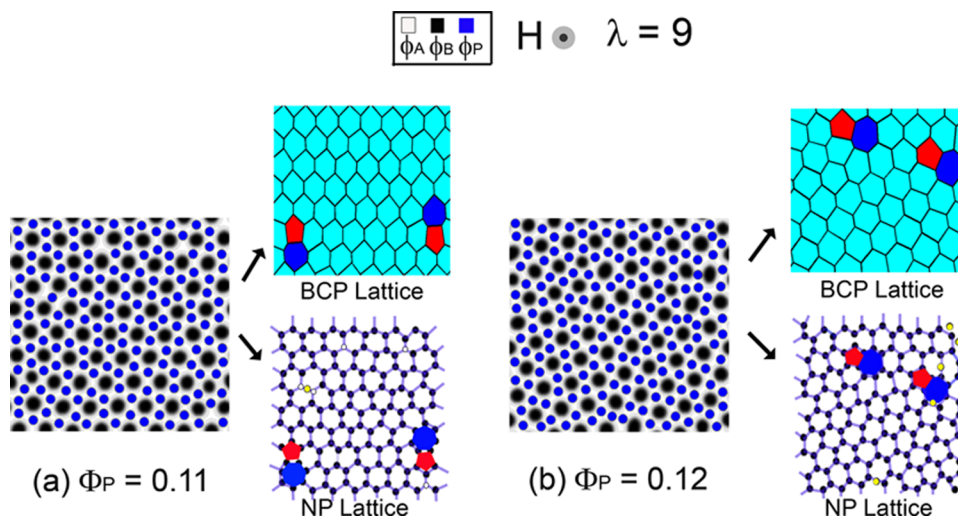


**Figure 2.** Effect of out-of-plane magnetic fields ( $\vec{H}$ ), when the nanoparticles are selective for the majority block;  $f = 0.7$ ,  $\chi_{AB}N = 0$ ,  $\chi_{BP}N = 30$ ,  $R_p = 0.5R_g$ , (a)  $\lambda = 9$ ,  $\Phi_P = 0.11$ , (b)  $\lambda = 9$ ,  $\Phi_P = 0.12$ . Red–blue polygon pairs denote dislocations in the block copolymer (BCP) and 5–7 defects in the nanoparticle (NP) lattice. Black empty circles denote one-vacancy defects in the nanoparticle lattice; yellow circles denote excess nanoparticles in the interstitial spaces.

nanocomposite. In the absence of an external magnetic field ( $\lambda = 0$ ), the superparamagnetic nanoparticles behave like nonmagnetic nanoparticles due to the absence of any remnant magnetic dipole moments. Thus, in the absence of an external magnetic field ( $\lambda = 0$ ), nanoparticles that have selective surface interactions ( $\chi_{AB}N = 0$ ,  $\chi_{BP}N = 30$ ) show behavior consistent with established results for block copolymer/nonmagnetic nanoparticle composites,<sup>13,16,17,25</sup> as seen in Figures 1a–e and in the Supporting Information, Figure S1. When the nanoparticles favor the majority block (Figure 1d,e;  $f = 0.7$ ), the increase in nanoparticle volume fraction does not affect the symmetry of the inverse hexagonal phase, although the hexagonal phase is distorted in some regions due to local structural frustration.

With superparamagnetic nanoparticles ( $\lambda = 9$ ), the orientation of the external magnetic field plays an important role in determining the morphology of the composite. Out-of-plane magnetic fields induce repulsive dipolar interactions resulting in formation of hexagonal arrays of nanoparticles. For nanoparticles selective for the minority block ( $f = 0.3$ ), the symmetry of the block copolymer lattice and the nanoparticle lattice match. When the lattice parameter of the nanoparticle structure matches the lattice parameter of the hexagonal phase block copolymer, hexagonal symmetry of the composite is preserved with minimal or no defects in the final morphology (Figure 1f). Using geometrical arguments, we can derive the optimum overall volume fraction of the nanoparticles for symmetry match to be  $\Phi_P^* = [(2\pi R_p^2)/(\sqrt{3}L_s^2)]$ , where  $L_s$  is the lattice constant of the nanoparticle-loaded hexagonal phase of the block copolymer (see Supporting Information, section A1). Since it is difficult to calculate the lattice constant of the nanoparticle loaded hexagonal phase a priori, to get an estimate of this optimum volume fraction, we assume that nanoparticles have a minor effect on the lattice constant of the hexagonal phase of the block copolymer (consistent with simulation results). This predicts that symmetry match might occur at  $\Phi_P^* = 0.057$  (for nanoparticles of radius  $R_p = 0.5R_g$ ); simulations show a symmetry match at about  $\Phi_P^* = 0.055$ . Although the final nanocomposite morphology looks similar in the two relatively small simulations shown in Figure 1a and f, faster

defect annihilation is expected in the presence of the external magnetic field due to the long-ranged nature of the dipolar interactions. Therefore, the inclusion of nanoparticles is anticipated to reduce the formation of defects when the particle loading is selected to be near this symmetry match. These symmetry matching conditions only apply when there is exactly one nanoparticle in each of the block copolymer minority nanodomains, which also requires commensurability between nanoparticle size ( $R_p$ ) and domain size (optimal nanoparticle size,  $R_p \sim 0.5\text{--}0.75R_g$ ). Figure S2 shows the effect of nanoparticle size on the morphology of an asymmetric block copolymer ( $f = 0.3$ ), in the presence of out-of-plane magnetic fields.

When the nanoparticle volume fraction is increased, the same morphological transition is observed (Figure 1g) as in the nonmagnetic nanoparticle case (Figure 1b). However, the morphology as a function of particle loading (Supporting Information, Figure S1) is unchanged from the nonmagnetic nanoparticle case, as the volume fraction is increased from 0.05 to 0.11. This indicates that dipolar interactions do not have a significant effect on the order-to-order phase transition (OOT), which is primarily caused by the swelling of the domains on addition of nanoparticles. However, this counterintuitive result is consistent with the fact that the energy of block copolymer self-assembly dominates the dipolar interaction strength for the values of parameters chosen in this study.

Block copolymer nanocomposites with symmetric composition ( $f = 0.5$ ) remain in a stripe phase even with the application of an out-of-plane magnetic field (Figure 1h). For a wide variety of different particle volume fractions, the repulsive dipolar interactions do not force the phase transition from lamellar (stripes) to hexagonal phase (dots) (see Supporting Information, Figure S3). Since the out-of-plane field does not orient the nanoparticles, symmetry is not broken, and the lamellar domains may orient in any direction. Morphological transitions from stripes to dots arise only because of the swelling of the domains (as seen in Supporting Information, Figure S3), as reported previously in the literature.<sup>13,16,17,24,25</sup>

When the superparamagnetic nanoparticles ( $\lambda = 9$ ) are selective for the majority block ( $f = 0.7$ ), they occupy the

interstitial spaces within the hexagonal dot morphology formed by the minority block in the presence of out-of-plane magnetic fields. As seen in Figure 2, for certain specific nanoparticle volume fractions; each nanoparticle has just three nearest neighbors, and they form a honeycomb lattice. This honeycomb lattice minimizes interparticle repulsive interactions by evenly spacing the particles throughout the block copolymer and places particles within the majority block of the hexagonal lattice at points farthest from the minority block domains, effectively reducing the decrease in entropy due to chain stretching in the majority block. Interparticle repulsive interactions, induced by out-of-plane magnetic fields, are critical to the formation of honeycomb lattices; the absence of the field results in a random dispersion of the nanoparticles in the majority block domains even at particle loadings optimal for honeycomb lattice formation (Supporting Information, Figure S4). Using geometrical arguments, we derive the optimum nanoparticle volume fraction at which a honeycomb lattice is formed to be  $\Phi_p^* = [(4\pi R_p^2)/(\sqrt{3}L_H^2)]$ , where  $L_H$  is the lattice constant of the nanoparticle-loaded hexagonal phase of block copolymer (see Supporting Information, Section A2).

This relationship is valid only for the case of a single nanoparticle occupying each interstitial space in the hexagonal lattice, which is dependent on the nanoparticle size. Assuming that the nanoparticles have only a minor effect on the block copolymer periodicity, we can estimate the optimum volume fraction for nanoparticles of radius  $R_p = 0.5R_g$  to be near 0.11. Simulations reveal the formation of a honeycomb lattice for nanoparticle volume fractions of  $\Phi_p = 0.11$  and  $\Phi_p = 0.12$  (Figure 2a and b); while higher and lower volume fractions do not show a honeycomb lattice (Supporting Information, Figure S4). For  $\Phi_p = 0.11$  and  $\Phi_p = 0.12$ , most nanoparticles have three-nearest neighbors (Figure 2). Honeycomb lattices are not observed for larger ( $R_p = 0.75R_g$ ) or smaller nanoparticles ( $R_p = 0.25R_g$ ) even at optimum volume fractions (Supporting Information, Figure S5). Larger nanoparticles ( $R_p = 0.75R_g$ ) distort the hexagonal structure of the block copolymer, while smaller nanoparticles ( $R_p = 0.25R_g$ ) are found dispersed in the majority block. Therefore, both the particle size and the particle volume fraction must be commensurate with the block copolymer lattice to achieve optimal field-induced ordering and formation of honeycomb lattices.

Defects in the block copolymer structure and the nanoparticle honeycomb lattice are collocated in the final structure. In the regions where dislocations (evident in five-sided red and seven-sided blue polygons in the BCP lattice, Figure 2a) occur in the block copolymer lattice, there are five and seven interstitial spaces in the block copolymer, each occupied by a single nanoparticle. This gives rise to 5–7 defects in the honeycomb lattice (as seen in five-sided red and seven-sided blue polygons in the NP lattice, Figure 2a).

In addition, for  $\Phi_p = 0.11$ , there are one-vacancy defects in the honeycomb lattice, shown as black empty circles (Figure 2a), due to an insufficient number of particles present to fill all of the interstitial spaces. In contrast, when the number of nanoparticles is slightly higher than the number of interstitial spaces in the block copolymer lattice (for  $\Phi_p = 0.12$ ), a few of the interstitial spaces tend to accommodate two particles instead of just one, without distorting the overall symmetry of the honeycomb lattice (as seen by yellow circles in the NP lattice of Figure 2b).

When the orientation of the magnetic field is changed to in-plane, the field causes chaining of nanoparticles, resulting in

stretching of A domains along the field direction for  $f = 0.3$  (Figure 1k). At higher nanoparticle volume fractions (Figure 1l), the persistence length of the nanoparticle chains increases, and the stripe phase is predominantly observed for  $\Phi_p > 0.11$  (see Supporting Information, Figure S6). For  $f = 0.5$  with an in-plane magnetic field (Figure 1m), extensive previous studies<sup>21,24</sup> have clearly demonstrated the ability of the field to induce particle chaining and block copolymer alignment.

When the nanoparticles are selective for the majority block ( $f = 0.7$ ), the hexagonal symmetry of the minority block is preserved in the presence of in-plane magnetic fields because the domains of the minority block are not stretched in the field direction (Figure 3). To accomplish this, the block copolymer

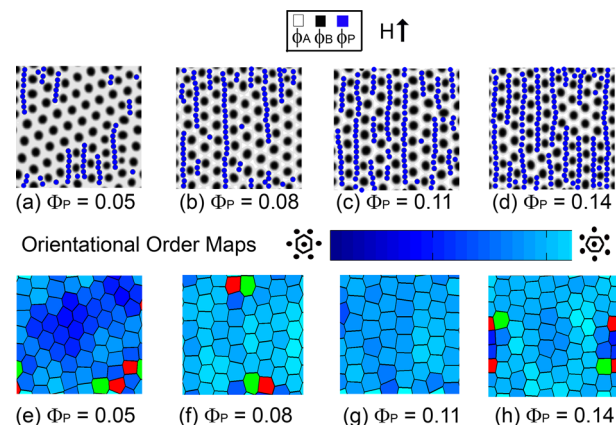


**Figure 3.** Orientational alignment of hexagonal phase of the minority block (B) by chaining of nanoparticles sequestered in the majority block (A) in the direction of external magnetic field ( $\vec{H}$ ) along the  $y$  axis;  $\lambda = 9$ ,  $\chi_{BP}N = 30$ ,  $R_p = 0.5R_g$ , (a)  $\Phi_p = 0.05$ , (b)  $\Phi_p = 0.08$ , (c)  $\Phi_p = 0.1$ , (d)  $\Phi_p = 0.14$ . Red–green polygons refer to dislocations; Voronoi maps shaded with orientational order parameter, for the corresponding volume fractions are given in e–h.

lattice aligns with the  $\langle 100 \rangle$  direction parallel to the superparamagnetic chains, resulting in control over the orientational order of the hexagonal phase. However, the addition of nanoparticles results in distortion of the hexagonal phase of the block copolymer (see Supplemental Section A3) with a transition seen in the symmetry of block copolymer morphology from hexagonal to centered rectangular symmetry at higher nanoparticle volume fractions (Figure 3d). Nevertheless, the orientation of the centered rectangular phases is in the direction of the external magnetic field along the  $\langle 100 \rangle$  direction, evident from the orientational order maps (Figure 3g). Beyond a critical volume fraction ( $\Phi_p^{\max}$ ), structural frustration of the block copolymer due to dynamic confinement between parallel nanoparticle chains with spacing less than the lattice spacing causes complete distortion in the hexagonal phase of the block copolymer. For *single* nanoparticle chains confined between minority domains of the block copolymer matrix, the maximum volume fraction beyond which distortion of the hexagonal phase of block copolymer becomes significant can be derived. Using geometrical arguments, we derive this critical volume fraction to be  $\Phi_p^{\max} = [(\pi R_p)/(\sqrt{3}L_1)]$  where  $L_1$  is the lattice constant of the nanoparticle-loaded hexagonal phase of the block copolymer (see Supporting Information, Section A4). For a nanoparticle radius of  $R_p = 0.5R_g$ , the maximum volume fraction beyond which a complete distortion of the hexagonal/centered rectangular phases occurs is around

0.18. The alignment of the hexagonal/centered rectangular phase at this volume fraction can be seen in Supporting Information, Figure S7.

To summarize, dipolar interactions in superparamagnetic nanoparticles are demonstrated to have a large effect on the morphology of block copolymer nanocomposites. The materials display a variety of transitions based on field orientation, volume fraction of block copolymer, nanoparticle size, and nanoparticle loading. Matching of both the symmetry and characteristic spacing of the structures formed by the superparamagnetic nanoparticles and the block copolymers enables improvement of block copolymer ordering, while a mismatch in structures drives phase transitions between poorly ordered phases. In the case of asymmetric copolymers with nanoparticles selective for the minority block, an out-of-plane magnetic field may be used to drive the nanoparticles into a hexagonal lattice that can reduce defects in the block copolymers. When the nanoparticles favor the majority block of an asymmetric block copolymer, application of an out of plane field leads to the formation of honeycomb lattices. Alternately, an in-plane field will produce superparamagnetic nanoparticle chains that can be used to orient the hexagonal phase of the block copolymer, provided the nanoparticles are selective for the majority block and are of appropriate size.

## ■ ASSOCIATED CONTENT

### 📄 Supporting Information

Additional simulation results and geometrical analysis. This material is available free of charge via the Internet at <http://pubs.acs.org>.

## ■ AUTHOR INFORMATION

### Corresponding Author

\*E-mail: [tahatton@mit.edu](mailto:tahatton@mit.edu) (T.A.H.); [bdolsen@mit.edu](mailto:bdolsen@mit.edu) (B.D.O.).

### Notes

The authors declare no competing financial interest.

## ■ ACKNOWLEDGMENTS

The authors would like to thank Arijit Bose, Christopher Lam, Mitchell Wang, and Charlotte Stewart-Sloan for their helpful discussions. The authors would also like to thank Cabot Corporation for funding this project.

## ■ REFERENCES

- (1) Balazs, A. C.; Emrick, T.; Russell, T. P. *Science* **2006**, *314* (5802), 1107–1110.
- (2) Bockstaller, M. R.; Mickiewicz, R. A.; Thomas, E. L. *Adv. Mater.* **2005**, *17* (11), 1331.
- (3) Xu, C.; Ohno, K.; Ladmiral, V.; Composto, R. J. *Polymer* **2008**, *49* (16), 3568.
- (4) Bockstaller, M.; Kolb, R.; Thomas, E. L. *Adv. Mater.* **2001**, *13* (23), 1783.
- (5) Fink, Y.; Urbas, A. M.; Bawendi, M. G.; Joannopoulos, J. D.; Thomas, E. L. *J. Lightwave Technol.* **1999**, *17* (11), 1963.
- (6) Buxton, G. A.; Balazs, A. C. *Phys. Rev. E* **2003**, *67* (3), 031802.
- (7) Huh, J.; Ginzburg, V. V.; Balazs, A. C. *Macromolecules* **2000**, *33* (21), 8085.
- (8) Lee, J.-Y.; Thompson, R. B.; Jasnow, D.; Balazs, A. C. *Phys. Rev. Lett.* **2002**, *89* (15), 155503.
- (9) Matsen, M. W.; Thompson, R. B. *Macromolecules* **2008**, *41* (5), 1853.
- (10) Pryamitsyn, V.; Ganesan, V. *Macromolecules* **2006**, *39* (24), 8499.

(11) Thompson, R. B.; Ginzburg, V. V.; Matsen, M. W.; Balazs, A. C. *Macromolecules* **2002**, *35* (3), 1060.

(12) Chiu, J. J.; Kim, B. J.; Kramer, E. J.; Pine, D. J. *J. Am. Chem. Soc.* **2005**, *127* (14), 5036.

(13) Yeh, S.-W.; Wei, K.-H.; Sun, Y.-S.; Jeng, U. S.; Liang, K. S. *Macromolecules* **2005**, *38* (15), 6559.

(14) Alexander, I. C.; Anna, C. B. *J. Chem. Phys.* **2003**, *119* (6), 3529–3534.

(15) Gaines, M. K.; Smith, S. D.; Samseth, J.; Bockstaller, M. R.; Thompson, R. B.; Rasmussen, K. Å.; Spontak, R. J. *Soft Matter* **2008**, *4* (8), 1609–1612.

(16) Pan, Q.; Tong, C.; Zhu, Y. *ACS Nano* **2011**, *5* (1), 123.

(17) Sides, S. W.; Kim, B. J.; Kramer, E. J.; Fredrickson, G. H. *Phys. Rev. Lett.* **2006**, *96* (25), 250601.

(18) Kim, J. U.; O'Shaughnessy, B. *Phys. Rev. Lett.* **2002**, *89* (23), 238301.

(19) Lee, J. Y.; Shou, Z.; Balazs, A. C. *Phys. Rev. Lett.* **2003**, *91* (13), 136103.

(20) Kang, H.; Detcheverry, F. A.; Mangham, A. N.; Stoykovich, M. P.; Daoulas, K. C.; Hamers, R. J.; Muller, M.; de Pablo, J. J.; Nealey, P. F. *Phys. Rev. Lett.* **2008**, *100* (14), 148303.

(21) He, G.; Balazs, A. C. *J. Comput. Theor. Nanosci.* **2005**, *2* (1), 99.

(22) Yethiraj, A. *Soft Matter* **2007**, *3* (9), 1099–1115.

(23) Hammond, M. R.; Dietsch, H.; Pravaz, O.; Schurtenberger, P. *Macromolecules* **2010**, *43* (20), 8340.

(24) Raman, V.; Bose, A.; Olsen, B. D.; Hatton, T. A. *Macromolecules* **2012**, *45* (23), 9373.

(25) Kim, B. J.; Chiu, J. J.; Yi, G. R.; Pine, D. J.; Kramer, E. J. *Adv. Mater.* **2005**, *17* (21), 2618.